Phase Separation in Microcapsule Membranes Composed of Soybean Lecithin, Cholesterol, Stearic Acid and Polyvinylpyrrolidone

Kaori JONO,*[,a] Hideki ICHIKAWA,[a] Yoshinobu FUKUMORI,[a] Ryuichi KANAMORI,[b] Yasuji TSUTSUMI,[b] Katsuko MURATA,[c] Atsuko MORIMOTO,[c] and Kenji NAKAMURA[c]

Faculty of Pharmaceutical Sciences, Kobe Gakuin University,[a] Arise, Ikawadani-cho, Nishi-ku, Kobe 651–21, Japan, Pharmaceutical Department, Itami Municipal Hospital,[b] Koya-ike 1–100, Itami, Hyogo 664, Japan, and Department of Radiology, Faculty of Medicine, Osaka City University,[c] 1–5–7 Asahi-cho, Abeno-ku, Osaka 545, Japan.
Received August 11, 1995; accepted October 20, 1995

A phase diagram of a soybean lecithin (SL)–cholesterol (CH)–stearic acid (SA) system incorporating 42% polyvinylpyrrolidone was estimated by differential scanning calorimetry (DSC), X-ray diffractometry (XRD) and polarizing microscopy in order to relate it to the dissolution and disintegration properties of microcapsules whose membranes consisted of these compounds. At the weight ratio of SL:CH=4:1, SL:SA=4:1 or SL:CH:SA=3:1:1, SL liquid crystalline phase (SL(LCP)) dissolved the maximum amount of CH and/or SA without any other crystalline phases detected on DSC and XRD. The existence of SL(LCP) was confirmed by observation under polarizing microscope: mixtures remained anisotropic over 20—90 °C or SA-containing anisotropic phases became isotropic at 70—80 °C without any peaks on DSC. With increase in CH and/or SA, these were separated from SL(LCP) dissolving CH and/or SA. The separated CH (CH(c)) was found to have the same crystalline structure as the parent CH from XRD. The separated SA, in contrast, showed two types of XRD patterns: one had the same pattern as the parent SA (SA(c)) and the other had a pattern with some peaks shifted to shorter spacings (SA(c')). The mixtures gave a phase diagram with six regions, each of which had the following phase(s): 1) SL(LCP); 2) SL(LCP) and CH(c); 3) SL(LCP), CH(c) and SA(c'); 4) CH(c), SA(c') and SA(c); 5) SA(c) and SA(c'); 6) SL(LCP) and SA(c'). It was not clear whether SL(LCP) was present in the fourth and fifth zones or not.

Key words microcapsule membrane; phase separation; lecithin; cholesterol; stearic acid; polyvinylpyrrolidone

In a previous study,[1] a soybean lecithin (SL) and its mixtures with additives were applied to delay and prolong the release of a water-soluble drug as membrane materials of microcapsules. It was demonstrated that such a system containing lecithin exhibited a sensitive hydration, followed by a short-term controlled release. This utilization of lecithin as a main component of the microcapsule membrane was different from such traditional uses as in coprecipitates and solid dispersions to improve the solubility and dissolution rate of poorly water-soluble drugs,[2] or in suppositories containing lecithin as a minor component to sustain the release of water-soluble drugs.[3]

A microcapsule was designed to be composed of a lactose core, a drug-layer of carbazochrome sodium sulfonate (CCSS, a model drug), SL, cholesterol (CH), stearic acid (SA) and polyvinylpyrrolidone (PVP) and a coat of SL, CH, SA and PVP. The release properties evaluated at 37 °C in a 0.9% saline solution by a column method[4] seemed to be controlled by the swelling and/or the hydration of the membrane as had been expected. When the coat lacked either or both CH and SA, the microcapsules showed a rapid burst in CCSS release. However, the release of CCSS exhibited a short-term delayed and subsequently prolonged profile when the coat was composed of all four components; the release properties were sensitive to the composition of the coat and the coating level. Then, the microcapsules coated with a SL–CH–SA mixture (5:5:2(42)) of 5:5:2 weight ratio containing 42% PVP based on this mixture showed a strongly prolonged profile.

When the membrane materials in anhydrous state were characterized by differential scanning calorimetry (DSC) and X-ray diffractometry (XRD), and microcapsules immersed in a dissolution medium were observed by polarizing microscopy, the above four-component mixture (5:5:2(42)) exhibited separation of a CH and a SA crystalline phase and formation of the swellable membrane, leading to a delayed and prolonged release of the drug. Although possible interactions of lecithin with CH and SA were discussed previously,[1] their detail remains unclear.

A ternary phase diagram has often been used to study three component systems.[5,6] For example, a diagram of the drug–oil–surfactant system or oil–surfactant–water system was drawn to find the optimum composition for microemulsion or self-emulsification. Similarly, a phase diagram of the SL–CH–SA system incorporating 42% PVP will also be useful in optimizing membrane formulations for effective treatments, for example, in chemoembolization and neutron-capture therapy, if it can be related to the drug release and the degradation properties of microcapsules.[1]

The present study was designed to elucidate phase separation in anhydrous SL membranes containing CH, SA and PVP in relation to the drug release from their microcapsules. The compositions were widely changed and then DSC, XRD and polarizing microscopy were carried out to draw a phase diagram.

Experimental

Materials SL (CP reagent grade, phosphatidylcholine of about 30%, phospholipids of 95% at the minimum) was purchased from Nacalai Tesque, Inc. SL contained 39% phosphatidylcholine, 33% phosphatidylethanolamine, 26% phosphatidylinositol and 2% of two kinds of unknown phospholipids as phospholipids, when analyzed by thin-layer chromatography and quantitative analysis of phosphate using

* To whom correspondence should be addressed.

the Rouser method.[7] CH (GP grade), SA (GP grade), PVP (K30, MW=40000, EP reagent grade), methylene chloride and ethanol were used as purchased from Nacalai Tesque, Inc. without purification.

DSC Anhydrous samples were prepared as previously reported.[1] The procedure was simply as follows: 500 mg of membrane materials was dissolved in 50 ml of methylene chloride–ethanol (1 : 1), the solvent was then evaporated by a rotary vacuum evaporator at a temperature below 30 °C and, subsequently, the residue was dried in a vacuum overnight at room temperature.

A differential scanning calorimeter (Shimadzu, DSC-50), equipped with a thermal analyzer (Shimadzu, TA-50WS) on a computer for process controlling, data collection and evaluation, was used. The onset temperatures, taken as the points of intersections of the tangents to the leading edge of the endotherm and the baseline, of the heating thermograms were considered the temperatures of the peaks. The anhydrous powdered sample of 6—7mg, except for SA, 1.65 mg, was loaded into an aluminum sample pan, crimped and heated at a rate of 5 °C/min under a nitrogen flow of 30 ml/min and a thermogram was recorded over the temperature range of −30 to 110 °C.

XRD X-ray diffraction patterns were recorded with a Rigakudenki X-ray diffractometer, Miniflex 2005 (Ni filter, CuK_α, 30 kV, 10 mA; time constant, 1 s; scanning rate, 2 degree/min). Anhydrous powdered samples were prepared in the same manner as those in DSC.

Polarizing Microscopy An Olympus POM polarizing microscope was used with a heating stage (MHS, Union Optical). Samples prepared in the same manner as those in DSC were observed in the temperature range of 20 to 90 °C.

Results

SL–CH Mixtures Incorporating 42% PVP DSC thermograms (Fig. 1A) and XRD patterns (Fig. 1B) of SL–CH mixtures incorporating 42% PVP are shown in Fig. 1. The DSC curve of CH was little affected by the addition of PVP (Fig. 1A a, b). The endothermic peak at 36 °C attributable to a separated CH[1] could be seen on the thermogram when the content of CH was 50% (1 : 1 : 0(42)) or more (Fig. 1A b—d). At 20% content this endothermic peak was still detectable (4 : 1 : 0(42), Fig. 1A e) when measured at a higher sensitivity, but at 17% content it was not (8.3 : 1.7 : 0(42), Fig. 1A f). A crystalline CH phase (CH(c)) was seen at 20% or more of CH content on XRD patterns (Fig. 1B b—e), consistent with DSC studies. XRD pattern of the phase seemed essentially the same as those of pure CH (0 : 1 : 0(0)) and 0 : 1 : 0(42) (Fig. 1B a, b).

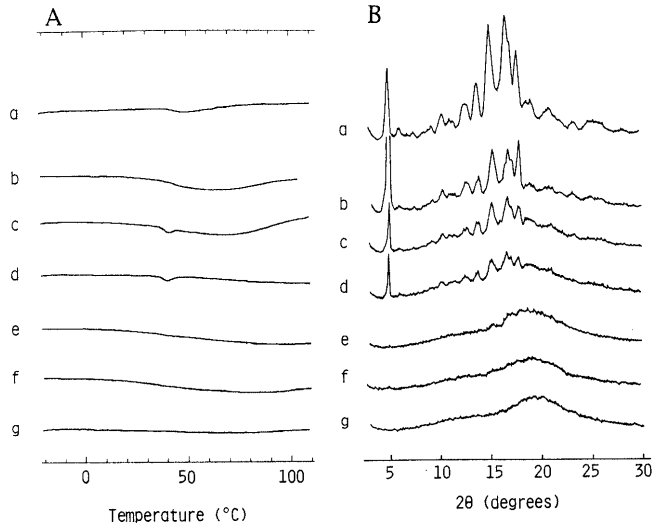

Fig. 1. DSC Thermograms (A) and XRD Patterns (B) of Anhydrous SL–CH Mixtures Incorporating 42% PVP

The weight ratio of SL, CH and SA (PVP, %): a, 0 : 1 : 0 (0); b, 0 : 1 : 0 (42); c, 1 : 2 : 0 (42); d, 1 : 1 : 0 (42); e, 4 : 1 : 0 (42); f, 8.3 : 1.7 : 0 (42); g, 1 : 0 : 0 (42).

SL–SA Mixtures Incorporating 42% PVP DSC thermograms (Fig. 2A) and XRD patterns (Fig. 2B) of SL–SA mixtures incorporating 42% PVP are shown in Fig. 2. Addition of PVP to SA broadened the endothermic peak at 67 °C, which was attributable to melting of SA, and lowered the transition temperature to 50 °C (0 : 0 : 1(42), Fig. 2A b). The broadened peaks were detected without change in the transition temperature, but with reduction in their peak area, as the SA content decreased to 20% (16 : 0 : 4(42), Fig. 2A j); below 20% the peak was undetectable (5 : 0 : 1(42), Fig. 2A k). On XRD patterns, when the SA content increased, all SA was dissolved in SL below its content of 20% (Fig. 2B k). At 20 or more % (Fig. 2B b—j), a crystalline SA phase was separated, but the XRD pattern was different from those of pure SA (0 : 0 : 1(0)) and of 0 : 0 : 1(42) (Fig. 2B a, b): the sharp peaks at $2\theta = 4.1, 6.1, 8.1, 10.1$ and 14.1 with both 0 : 0 : 1(0) and 0 : 0 : 1(42) mixtures shifted to larger $2\theta = 4.4, 6.6, 8.8, 11.0$ and 15.3, respectively, with the SL–SA mixtures. This suggested that the SA phase separated in the SL–SA mixtures, designated as SA(c′) in the following, might be different in a molecular packing from SA alone and SA with PVP.

CH–SA Mixtures Incorporating 42% PVP DSC thermograms (Fig. 3A) and XRD patterns (Fig. 3B) of CH–SA mixtures incorporating 42% PVP are shown in Fig. 3. With increase in CH added to SA, the endothermic peak at 50 °C, which was attributable to the melting

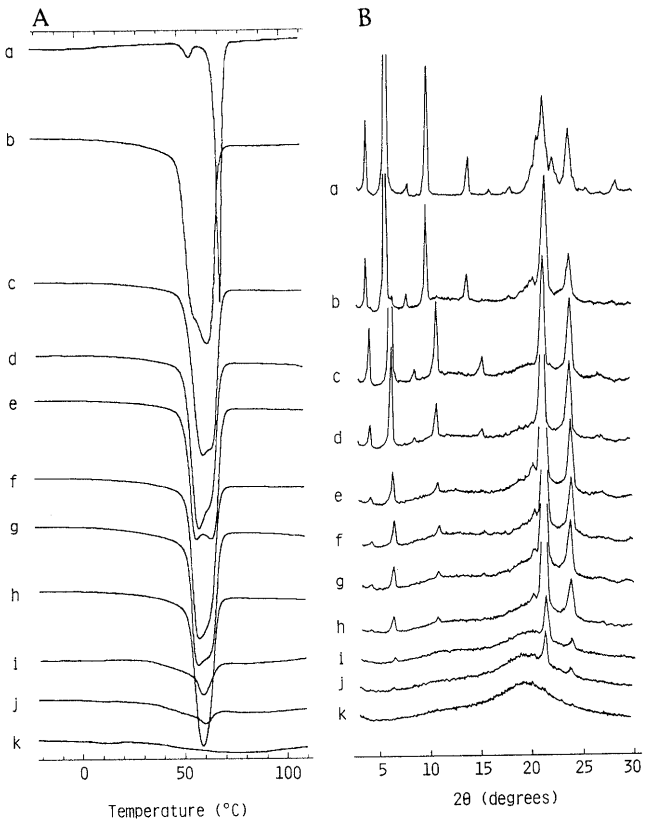

Fig. 2. DSC Thermograms (A) and XRD Patterns (B) of Anhydrous SL–SA Mixtures Incorporating 42% PVP

The weight ratio of SL, CH and SA (PVP, %): a, 0 : 0 : 1 (0); b, 0 : 0 : 1 (42); c, 0.5 : 0 : 19.5 (42); d, 1 : 0 : 19 (42); e, 2 : 0 : 18 (42); f, 3 : 0 : 17 (42); g, 4 : 0 : 16 (42); h, 6 : 0 : 14 (42); i, 5 : 0 : 2 (42); j, 16 : 0 : 4 (42); k, 5 : 0 : 1 (42).

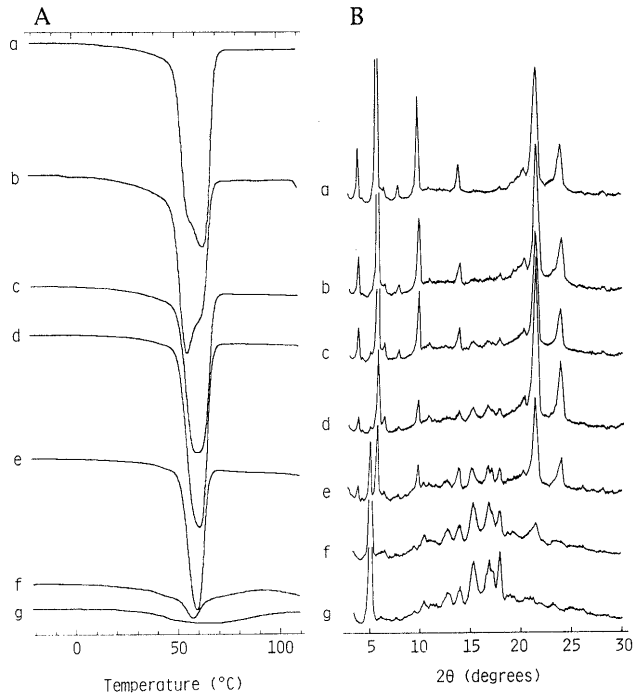

Fig. 3. DSC Thermograms (A) and XRD Patterns (B) of Anhydrous CH–SA Mixtures Incorporating 42% PVP

The weight ratio of SL, CH and SA (PVP, %): a, 0:0:1 (42); b, 0:1:9 (42); c, 0:1.5:8.5 (42); d, 0:2:8 (42); e, 0:1:1 (42); f, 0:9:1 (42); g, 0:1:0 (42).

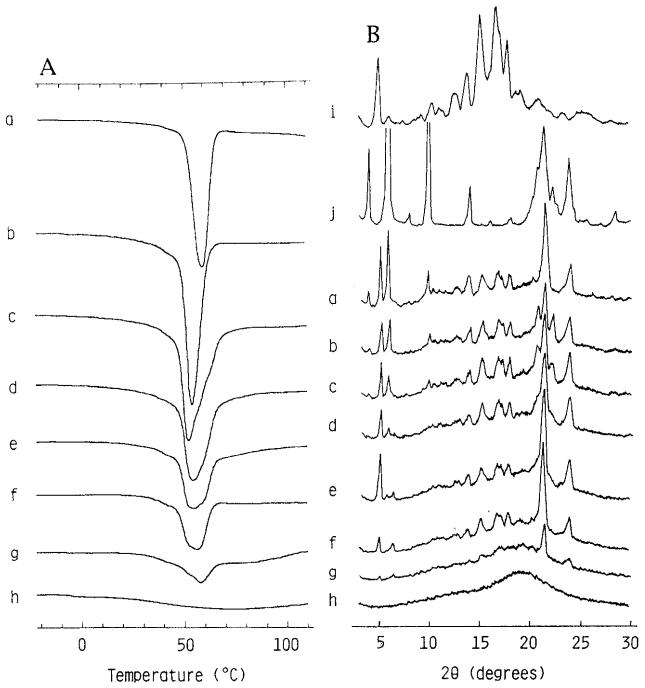

Fig. 4. Effects of SL on DSC Thermograms (A) and XRD Patterns (B) of Anhydrous $X:5:5$ (42) SL–CH–SA Mixtures Incorporating 42% PVP

The weight ratio of SL, X, was changed in $X:5:5$ (42): a, $X=0$; b, $X=0.5$; c, $X=1$; d, $X=2$; e, $X=3$; f, $X=4$; g, $X=12.5$; h, $X=45$; i, CH; j, SA.

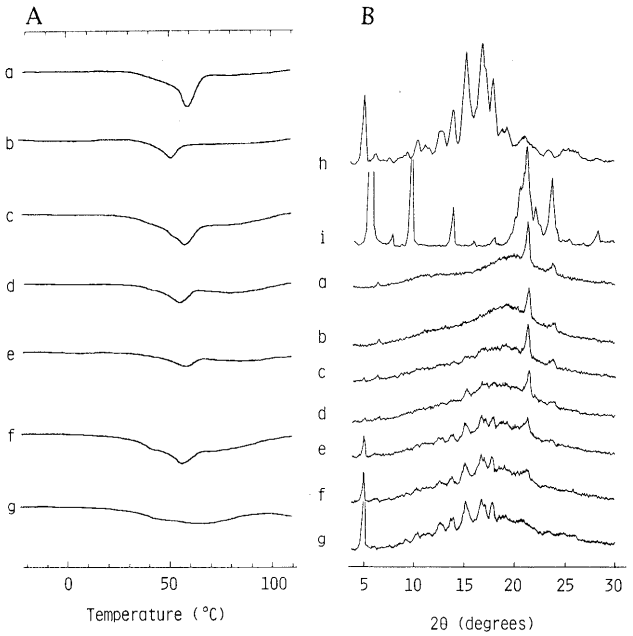

Fig. 5. Effects of CH on DSC Thermograms (A) and XRD Patterns (B) of Anhydrous $5:Y:2$ (42) SL–CH–SA Mixtures Incorporating 42% PVP

The weight ratio of CH, Y, was changed in $5:Y:2$ (42): a, $Y=0$; b, $Y=1$; c, $Y=2$; d, $Y=3$; e, $Y=5$; f, $Y=7$; g, $Y=16$; h, CH; i, SA.

of SA, became smaller; however, it was clearly detectable even at 10% of SA content (0:9:1(42), Fig. 3A f). The endothermic peak of CH(c) was barely detected even at a high sensitivity when the CH content was at 50% (0:1:1(42)) or more % (Fig. 3A e—g). On XRD pattern, when the CH content increased, all CH was dissolved when the content was less than 15% (Fig. 3B b). Above 15% (Fig. 3B c—g), the CH(c) phase was separated; the XRD pattern was not different from CH alone, CH with PVP or CH(c) in the SL–CH mixtures (Fig. 1B). XRD pattern of the SA phase had peaks similar to those of pure SA (0:0:1(0), Fig. 2B a). This SA phase, designated as SA(c) in the following, seemed to be different from SA(c′).

SL–CH–SA Mixtures Incorporating 42% PVP DSC thermograms (Fig. 4A) and XRD patterns (Fig. 4B) of SL–CH–SA mixtures incorporating 42% PVP are shown in Fig. 4, when SL content (X) was changed at $X:5:5$(42). The endothermic peak at $X=0$ (0:1:1(42), Fig. 4A a) was broader than that of SA alone (0:0:1(0), Fig. 2A a), due to the incorporated PVP and/or CH. With increase in X, the peak broadened further, and then disappeared at $X=45$ (45:5:5(42), Fig. 4A h). The XRD patterns of mixtures of $X:5:5$(42) clearly demonstrated the difference between SA(c) and SA(c′), as shown in Fig. 4B. When the SL content was lower than $X=4$ (Fig. 4B b—e), except for $X=0$, the peaks were observed at $2\theta=6.1$ and 6.6.

DSC thermograms (Fig. 5A) and XRD patterns (Fig. 5B) of SL–CH–SA mixtures incorporating 42% PVP are shown in Fig. 5, when CH content (Y) was increased at the ratio of $5:Y:2$(42). The XRD pattern for 5:0:2(42) ($Y=0$, Fig. 5B a) indicated that the separated SA crystalline phase was SA(c′). With increase in Y, CH(c) began to separate at $Y=2$ (5:2:2(42), Fig. 5B c); then, the crystalline structure of separated CH phase seemed identical to that of CH alone (Fig. 5B h). This corresponded to the occurrence of a small shoulder at 38 °C at $Y=2$ or more on DSC thermograms (Fig. 5A c—g). It was clear from XRD that the main peaks at 47—55 °C on the thermograms at $Y=0$—7 (Fig. 5A a—f) originated from the separation of SA(c′).[1] At $Y=16$

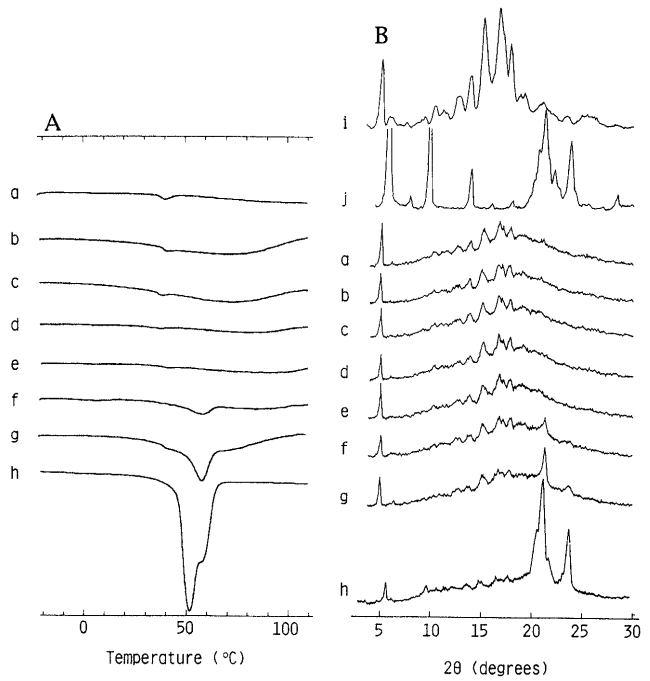

Fig. 6. Effects of SA on DSC Thermograms (A) and XRD Patterns (B) of Anhydrous 5 : 5 : Z (42) SL–CH–SA Mixtures Incorporating 42% PVP

The weight ratio of SA, Z, was changed in 5 : 5 : Z (42): a, $Z=0$; b, $Z=0.25$; c, $Z=0.5$; d, $Z=0.75$; e, $Z=1$; f, $Z=2$; g, $Z=3$; h, $Z=20$; i, CH; j, SA.

(5 : 16 : 2(42)), the separation of SA(c′) was only slightly detected on the XRD pattern (Fig. 5B g), along with broadening of the main peak on the DSC thermogram (Fig. 5A g).

DSC thermograms (Fig. 6A) and XRD patterns (Fig. 6B) of SL–CH–SA mixtures incorporating 42% PVP are shown in Fig. 6, when SA content (Z) was increased at 5 : 5 : Z(42). Membrane materials became very hygroscopic, even when such a small amount of SA as $Z=0.25$ was added; this induced a broad peak over 0—100 °C, possibly originating from water-adsorbed PVP (Fig. 6A b).[1] With increase in Z, SA began to be separated at $Z=2$ (5 : 5 : 2(42)), as clear from the XRD pattern (Fig. 6B f), whereas a separation of CH(c) could be observed in every case (Fig. 6B). These corresponded to appearances of peaks at 50—51 °C due to the SA separation and at 36—39 °C due to the CH(c) separation on DSC thermograms (Fig. 6A). It was observed on XRD that only SA(c′) was separated at $Z=2$ and 3 (Fig. 6B f, g), and SA(c′) and SA(c) coexisted at $Z=20$ (Fig. 6B h).

Phase Diagram of SL–CH–SA–PVP Systems An estimated phase diagram of the SL–CH–SA system containing 42% PVP in anhydrous state is shown in Fig. 7. All compositions are expressed in total weight percent of SL, CH and SA. The vertexes of the diagram indicate 100% of SL, CH and SA, respectively. Each plot shows the measured points to determine the boundaries and three broken lines show the compositions at X : 5 : 5, 5 : Y : 2 and 5 : 5 : Z. At points around the boundaries, physical mixtures with the same components were also used to confirm that the disappearance of peaks was not due to the detection limits in both DSC and XRD studies. The obtained diagram indicated that there were six different

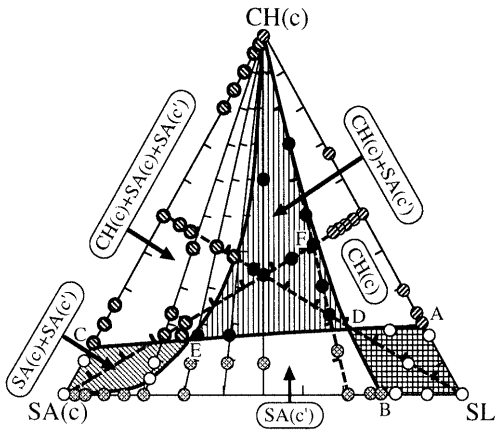

Fig. 7. Phase Diagram for Anhydrous SL–CH–SA System Incorporating 42% PVP

The weight ratio of SL, CH and SA (PVP, %): A, 8.2 : 1.8 : 0 (42); B, 4 : 0 : 1 (42); C, 0 : 3 : 17 (42); D, 4 : 1 : 1 (42); E, 5 : 3 : 10 (42); F, 5 : 5 : 2 (42). Separation of crystalline phase(s) detected by DSC or XRD: zone SL–A–D–B, none; zone CH–A–D, CH; zone SA(c)–B–D–E, SA(c′); zone SA(c)–E–C, SA(c) and SA(c′); zone CH–C–E, CH, SA(c) and SA(c′); zone CH–D–E, CH and SA(c′).

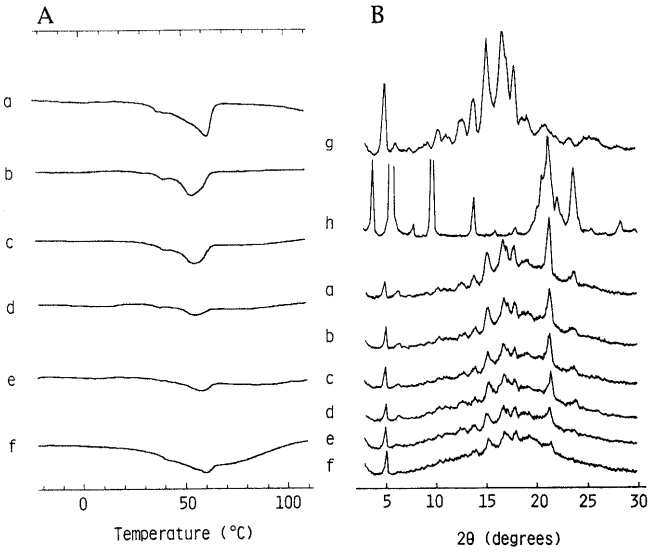

Fig. 8. Effects of PVP on DSC Thermograms (A) and XRD Patterns (B) of Anhydrous 5 : 5 : 2 (P) SL–CH–SA Mixtures Incorporating PVP

The weight percent of PVP, P, was changed in 5 : 5 : 2 (P): a, $P=0$; b, $P=10$; c, $P=20$; d, $P=30$, e, $P=42$; f, $P=50$; g, CH; h, SA.

states of mixing with the following phase(s) crystalline on XRD: no crystalline phase in zone SL–A–D–B; CH(c) in zone CH–A–D; CH(c) and SA(c′) in zone CH–D–E; CH(c), SA(c) and SA(c′) in zone CH–C–E; SA(c) and SA(c′) in zone SA–C–E; SA(c′) in zone SA–B–D–E. It was also found that in the binary systems CH could be dissolved in SL and SA up to 20% and 15%, respectively, and SA in SL up to 20%.

Effect of PVP on Phase Separation DSC thermograms (Fig. 8A) and XRD patterns (Fig. 8B) of SL–CH–SA mixtures are similarly shown in Fig. 8, when PVP content (P, % against the total weight of SL, CH and SA) was increased at 5 : 5 : 2(P). Thermograms had two endotherms at 35—38 and 47—50 °C (Fig. 8A) originating from separated CH and SA, respectively; the latter was seen at 57 °C at $P=0$ (5 : 5 : 2(0), Fig. 8A a). Their height decreased with increase in P, but no meaningfully different phase transition was noted. The XRD patterns were also

little affected by increase in PVP content, except for decrease in their peak height (Fig. 8B).

Discussion

A phase diagram was drawn for the SL–CH–SA system incorporating 42% PVP, because the system without PVP could not work as a membrane of microcapsules due to its low coating efficiency. The phase diagram was to be related with the disintegration and dissolution properties of the microcapsules.

In DSC thermogram of CH alone (0 : 1 : 0(0), Fig. 1A a), the endothermic peak at 40 °C is due to polymorphic change of CH.[1] Different temperatures have been reported for the polymorphic change.[8,9] The transition temperature in the present study agreed well with that reported by Spier and Senden.[9] It was not affected by the addition of 42% PVP (Fig. 1A b).

The endothermic peak of SA (Fig. 2A a) was lowered to 50 °C and broadened by the incorporation of 42% PVP (Fig. 2A b), though the transition of the physical mixture of SA and 42% PVP appeared at the same temperature, 67 °C, as that of SA alone with a similar peak shape (data not shown). Garti *et al.* reported that SA had three different crystalline forms termed A, B and C.[10] The differential thermal analysis (DTA) indicated that the A form transformed to the C form at 64 °C followed by a hardly measurable endotherm. The B form exhibited an endothermic phase transition to the C form at 54 °C (peak temperature in DTA), while the C form showed melting at 75 °C. The DSC thermogram of SA (0 : 0 : 1(0)) used in our study showed a small peak at 51 °C and a larger endothermic peak at 67 °C leading to melting (Fig. 2A a). In addition to DSC, XRD also suggested the SA used in our study was the B form, though there was a little difference only in peak intensity in the range of $2\theta = 20$ to 25, but not in peak position. The XRD pattern of SA incorporating 42% PVP (0 : 0 : 1(42)) suggested that the 0 : 0 : 1(42) mixture was also the B form (Fig. 2B b). On DSC, the transition of 0 : 0 : 1(42) mixture started at 51 °C, which was correctly the same as that with 0 : 0 : 1(0) mixture, though its endothermic peak was very broad. On a polarizing microscopy, SA incorporating 42% PVP (0 : 0 : 1(42)) was also anisotropic at 20 °C and started to melt into isotropic liquid around 47 °C corresponding to the DSC curve (Figs. 2A b, 3A a). These implied that the 0 : 0 : 1(42) mixture started the transition from the B form to the C form at 51 °C, but the melting of the C form occurred at a lower temperature due to the coexistence of PVP, leading to broadening of the transition peak.

With polarizing microscopy, SL incorporating 42% PVP (1 : 0 : 0(42)) was anisotropic at 20 °C and no change occurred in the range of 20—90 °C. Further, DSC exhibited no gel to liquid crystalline phase transition of SL used (Fig. 1A g). Therefore, it was reasonable to consider that SL having unsaturated acylic chains was a liquid crystalline phase at the temperatures herein studied: this SL liquid crystalline phase will be designated as SL(LCP) in the following.

According to the compositions of SL, CH and SA, the mixtures gave a phase diagram with six regions (Fig. 7). In zone SL–A–D–B, all of CH and SA seemed to be dissolved in SL, because the phase was amorphous on XRD (Figs. 1B f, g, 2B k, 4B h) and exhibited no transition peak on DSC (Figs. 1A f, g, 2A k, 4A h). In the dipalmitoylphosphatidylcholine (DPPC)–CH system in an excess of water, a pure DPPC and a DPPC–CH domain exist as phase-separated mixture below 20 mol% of CH.[11] In addition, SA also interacts with DPPC and forms a gel solid solution with 1 : 2 DPPC–SA stoichiometry in excess water.[12] In our case, there would be a potential for SL–CH and SL–SA domains to be formed in zone SL–A–D–B where all CH and SA would be dissolved in SL, if the mixture were hydrated in excess water. However, the anhydrous mixtures studied here did not exhibit such domains. For example, the mixture of 9 : 1 : 1(42) (Fig. 4A h, 4B h) in this zone was anisotropic at 20 °C with very little dark and opaque part which seemed not to be anisotropic. The anisotropic part changed to an isotropic phase at 70—80 °C without melting into a fluid liquid and without any transition peaks detected on DSC. This phenomenon was also observed at the same temperature when a small amount of SA was added to SL (Fig. 2A k, 2B k, on the line SL–B), though SL alone showed no melting below 90 °C. These indicated that the dissolution of SA in SL induced disappearance of SL(LCP) at 70—80 °C.

The maximum amounts of CH and/or SA that this SL phase could dissolve are shown by the boundaries SL–A–D–B in Fig. 7, where the weight ratios of points A, B and D are about 4 : 1 : 0, 4 : 0 : 1 and 3 : 1 : 1, respectively. The obtained value of 20% at point A was well consistent with the result (18%) reported by Bourges *et al.*[13]; but not with the 33% found by Khan and Tucker.[14] This would be because the lecithins used were different in acyl chain length, saturation and chemically heterogeneous nature especially since Khan and Tucker[14] used hydrogenated egg lecithin.

In zone CH–A–D, XRD and DSC indicated that CH(c) was separated (Fig. 6A, 6B). The mixture of 5 : 5 : 0(42) was observed to be anisotropic at 20—90 °C under the microscope. The mixture of 5 : 5 : 0.5(42) changed from the anisotropic to isotropic phase at around 75 °C with a slight amount of the anisotropic part remaining. This change was similar to that in zone SL–A–D–B, indicating that there was SL(LCP) containing SA. The remaining anisotropic part above 75 °C would be due to the separated CH(c).

Among the six different states of mixing in the estimated phase diagram, the most interesting zone was CH–D–E. This included the 5 : 5 : 2(42) mixture shown by point F in Fig. 7, which exhibited a desirable short-term controlled release property in the previous study.[1] In zone CH–D–E, CH(c) and SA(c′) were separated. The XRD pattern of SA(c′) was similar to that of C form reported by Garti *et al.*[10] In this zone, the mixtures were anisotropic at 20 °C under the microscope. The 5 : 5 : 3(42) and 5 : 5 : 5(42) mixtures ($Z = 3$, 5) began to melt around 45 °C and a transparent liquid then appeared with an opaque part remaining. The only possible phase that could melt at this temperature was SA(c′), because its melting temperature was 67 °C in the pure state (Fig. 2A a), but it could be lowered to 50 °C by concomitants. On the other hand, the

separation of CH(c) could not be confirmed in this zone by the microscopy, since the melted SA(c′) dissolved the other phases almost completely: this dissolution of the other phases in melted SA(c′) was reflected by broadening of the endothermic peak at about 50 °C on DSC (Figs. 4A—6A). As regards the 5:5:2(42) mixture, the separation of both CH and SA(c′) on DSC and XRD studies was clearly indicated (Fig. 5A e, 5B e), but there was no melting into a fluid liquid at around 45 °C specific with SA(c′). The 5:5:2(42) mixture completely changed from anisotropic to isotropic phase at about 75 °C as seen in zone CH–A–D, indicating the existence of SL(LCP) containing SA. This would be because the small amount of SA(c′) in the 5:5:2(42) mixture, very close to the border of CH–D, could not dissolve the other phases at around 45 °C. Further, the small area of peaks on DSC curves of the mixtures along X:5:5(42), 5:Y:2(42) and 5:5:Z(42) lines in zone CH–D–E indicated SL(LCP) to coexist together with SA(c′) and CH(c) (Figs. 4A—6A).

Zone CH–C–E had three separate crystalline phases: SA(c), SA(c′) and CH(c). The coexistence of SA(c) with SA(c′) was clearly shown by XRD patterns with the 2:5:5(42) and 3:5:5(42) mixtures (Fig. 4B d, e). The mixture in zone CH–C–E under the microscope was similar to that in zone CH–D–E: the mixture 5:5:15(42) in this zone was anisotropic at 20 °C and completely melted around 45 °C into a transparent isotropic liquid. This meant that the amount of SA(c) and SA(c′) would be sufficient to completely dissolve all the other phase(s); therefore, SL(LCP) could not be confirmed in this zone. Nor could any difference between SA(c) and SA(c′) be found under the microscope.

In zone SA–C–E, all CH dissolved, and SA(c) and SA(c′) were separated. The mixture in zone SA–C–E was also anisotropic at 20 °C under the microscope and melted around 45 °C, as seen with those in zones CH–D–E and CH–C–E. Therefore, the existence of SL(LCP) could not be confirmed.

In zone SA–B–D–E, only SA(c′) was separated. This zone was differentiated from zone SA–C–E by the absence of peaks of 2θ= 4.1, 6.1, 8.1, 10.1 and 14.1 of SA(c) on XRD. Mixtures in zone SA–B–D–E seen under the microscope were similar to that in zone SA–C–E. There was only partial melting separated SA(c′) around 50 °C with a low content of SA and an opaque part remained. An high content, on the other hand, all of the components were dissolved in the melted SA(c′). The area of peaks on DSC curves was very small in the right half of this region close to point B (Figs. 2A i, j, 5A a, b, 7). These suggested that SL(LCP) might exist in zone SA–B–D–E.

Another interesting observation in zone SA–B–D–E was that the SA(c) phase changed to SA(c′) with the addition of only a little SL to SA (0.5:0:19.5(42), Fig. 2A c, 2B c, 7); however, the SA(c) phase appeared again with the subsequent addition of a small amount of CH to the SL–SA mixture, as shown in the region close to the SA(c) vertex of the phase diagram (Fig. 7). These sensitive variations of the SA phase suggested that a minor amount of CH or SL might strongly affect the packing structure of SA molecules when they were precipitated from solutions.

Conclusion

The phase diagram of SL–CH–SA incorporating 42% PVP was estimated by DSC, XRD and polarizing microscopic studies. Two types of SA phases were detected on XRD: SA(c) with the same pattern as the parent SA and SA(c′) with some peaks shifted to spacings shorter than those of SA(c). The existence of SL(LCP) in each zone was confirmed based on the following microscopic observations: 1) the mixture was anisotropic at 20—90 °C; 2) the SA-containing mixture, which was anisotropic at 20 °C, became isotropic at 70—80 °C without any peaks on DSC. According to the proportions of SL, CH and SA, the mixtures gave a phase diagram with six regions, each of which had the following phase(s): 1) SL(LCP); 2) SL(LCP) and CH(c); 3) SL(LCP), CH(c) and SA(c′); 4) CH(c), SA(c′) and SA(c); 5) SA(c) and SA(c′); 6) SL(LCP) and SA(c′). It was not confirmed whether or not SL(LCP) was present in the fourth and fifth zones. However, there is a strong possibility that SA(c′) separated in zone CH–D–C might have the composition at point E and that the mixtures in zone CH–E–SA might have no SL(LCP). These points are still not clear, but will be interesting subjects to study. With regard to PVP, it seemed to have little meaningful effect on phase transition.

The physical states of systems containing lecithin are greatly changed by hydration as reported by many authors.[13,15] This change must be concerned with disintegration and drug release properties of microcapsules with the lecithin membranes. This is also a subject for future investigations.

Acknowledgment This work was supported in part by a grant-in-aid for cancer research (4—13) from the Japanese Ministry of Health and Welfare, a grant-in-aid for science research (05671798) from the Japanese Ministry of Education, Science and Culture, a grant-in-aid from the Hosokawa Powder Technology Foundation and a grant-in-aid for health science from Kobe Gakuin University.

References

1) Fukumori Y., Ichikawa H., Jono K., Tokumitsu H., Shimizu T., Kanamori R., Tsutsumi Y., Nakamura K., Murata K., Morimoto A., Tsubakimoto M., Nakatsuka H., Minakuchi K., Onoyama Y., *Chem. Pharm. Bull.*, **42**, 2604—2611 (1994).
2) *a*) Venkataram S., Rogers J. A., *J. Pharm. Sci.*, **73**, 757—761 (1984), *b*) *Idem*, *Drug Dev. Ind. Pharm.*, **11**, 223—238 (1985); *c*) Fujii M., Terai H., Mori T., Sawada Y., Matsumoto M., *Chem. Pharm. Bull.*, **36**, 2186—2192 (1988); *d*) Fujii M., Harada K., Yamanobe K., Matsumoto M., *ibid.*, **36**, 4908—4913 (1988); *e*) Fujii M., Harada K., Matsumoto M., *ibid.*, **38**, 2237—2241 (1990); *f*) Fujii M., Hasegawa J., Kitajima H., Matsumoto M., *ibid.*, **39**, 3013—3017 (1991); *g*) Vudathala G. K., Rogers J. A., *J. Pharm. Sci.*, **81**, 282—286 (1992); *h*) *Idem*, *ibid.*, **81**, 1166—1169 (1992); *i*) Fujii M., Hioki H., Nishi M., Henmi T., Nakao M., Shiozawa K., Matsumoto M., *Chem. Pharm. Bull.*, **41**, 1275—1278 (1993).
3) *a*) Nishihata T., Wada H., Kamada A., *Int. J. Pharm.*, **27**, 245—253 (1985); *b*) Nishihata T., Sudho M., Kamada A., Keigami M., Fujimoto T., Kamide S., Tatsumi N., *ibid.*, **33**, 181—186 (1986); *c*) Nishihata T., Keigami M., Kamada A., Fujimoto T., Kamide S., Tatsumi N., *ibid.*, **42**, 251—256 (1988).
4) Fukumori Y., Ichikawa H., Tokumitsu H., Miyamoto M., Jono K., Kanamori R., Akine Y., Tokita N., *Chem. Pharm. Bull.*, **41**, 1144—1148 (1993).
5) Charman S. A., Charman W. N., Rogge M. C., Wilson T. D., Dutko F. J., Pouton C. W., *Pharm. Res.*, **9**, 87—93 (1992).
6) Constantinides P. P., Scalart J-P., Lancaster C., Marcello J., Marks

G., Ellens H., Smith P. L., *Pharm. Res.*, **11**, 1385—1390 (1994).
7) Rouser G., Siakotos A. N., Fleisher S., *Lipids*, **1**, 85 (1966).
8) *a*) van Putte K., Skoda W., Petroni M., *Chem. Phys. Lipids*, **2**, 361—371 (1968); *b*) Loomis C. R., Shipley G. G., Small D. M., *J. Lipid Res.*, **20**, 525—535 (1979).
9) Spier H. L., van Senden K. G., *Steroids*, **6**, 871—873 (1965).
10) Garti N., Wellner E., Sarig S., *Cryst. Tech.*, **15**, 1303—1310 (1980).
11) McMullen T. P. W., McElhaney R. N., *Biochim. Biophys. Acta*, **1234**, 90—98 (1995).
12) Schullery S. E., Seder T. A., Weinstein D. A., Bryant D. A., *Biochemistry*, **20**, 6818—6824 (1981)
13) Bourges M., Small D. M., Dervichian D. G., *Biochim. Biophys. Acta*, **137**, 157—167 (1967).
14) Khan M. Z. I., Tucker I. G., *Chem. Pharm. Bull.*, **40**, 3056—3061 (1992).
15) *a*) Small D. M., Bourges M. C., Dervichian D. G., *Biochim. Biophys. Acta*, **125**, 563—580 (1966); *b*) Ladbrooke B. D., Williams R. M., Chapman D., *ibid.*, **150**, 333—340 (1968).